Battery Energy Storage Systems Providing Dynamic Containment Frequency Response Service

Xihai Cao, Jan Engelhardt, Charalampos Ziras, Mattia Marinelli, Nan Zhao

***Abstract*—Battery energy storage systems (BESS) have emerged as a critical component in maintaining power system stability through frequency regulation. Their rapid response and flexible characteristics have generated considerable interest among researchers. This study focuses on the provision of a fast frequency response service, known as Dynamic Containment Frequency Response (DCFR), in Great Britain (GB). It conducts a detailed assessment of BESS-based DCFR service for frequency regulation and State-of-charge (SOC) management, including the configuration constraints set out by the energy recovery rules and SOC management impact. A methodology is presented to investigate the performance of DCFR-based BESS in a power system, alongside a stability analysis focusing on the impact of the SOC management mechanism. The stability study investigates the potential influential factors of battery SOC management when providing DCFR via root locus. For simulation case studies, a power imbalance estimation method is utilized for gaining the input. Based on the stability analysis results, key BESS configuration parameters are examined in an integrated power system model: C-rate, SOC management range, ratio and target. Another influential factor, SOC management time delay, is also analyzed. Finally, a comparison between DCFR and the previous frequency regulation service, Enhanced frequency response (EFR), is conducted. The study reveals that improper SOC management in DCFR can lead to SOC oscillation, adversely affecting performance. However, with proper configuration, DCFR offers more favorable outcomes than EFR in terms of frequency quality, SOC levels, and battery degradation.**

***Index Terms*—Frequency response, battery energy storage system, power system, low inertia.**

Abbreviations

DCFR	Dynamic containment Frequency Response
BESS	Battery energy storage systems
EFR	Enhanced frequency response
ER	Energy recovery
FEC	Full equivalent cycles
GB	Great Britain
NGET	National Grid Electricity Transmission
PFR	Primary frequency response
RES	Renewable energy sources
REV	Response energy volume
SFR	Secondary frequency response
SOC	State-of-charge
SP	Settlement period
TSO	Transmission system operator

I. Introduction

THE need for decarbonization in recent years has resulted in a notable upsurge in the integration of Renewable energy sources (RES) in power systems, with renewables accounting for 50.9% of the total electricity generation in the UK during the first quarter of 2024 [1]. However, the low-inertia and intermittency of RES introduce challenges, such as more volatile frequency variation. Power system frequency is a critical factor indicating the balance between generation and demand, and requires regulation within specific limits. Various frequency response services, including Primary frequency response (PFR) and Secondary frequency response (SFR), are employed to achieve desirable frequency conditions.

However, the increasing penetration of non-synchronous renewable generation compromises conventional frequency regulation capabilities. To overcome this shortcoming, BESS offer a promising alternative solution due to their fast-responding, flexible, and scalable features [2]. Therefore, there is a growing interest in researching BESS for their potential to provide frequency regulation services. While the utilization of BESS for PFR has been widely discussed [3]–[5], fast frequency response services for BESS are emerging as new techniques to tackle frequency fluctuation. The Transmission system operator (TSO) in Ireland has developed fast frequency response services [6], while fast frequency reserve service is being implemented in Denmark to address frequency deviation in a prompter way [7]. However, both products are specifically tailored for under-frequency scenarios. On the other hand, services such as primary containment reserve and fast instantaneous reserves are deployed in Germany and New Zealand [8], [9], enabling providers the ability to deliver the support in a symmetric manner, but fast instantaneous reserves do not include any energy recovery rules suitable for energy-limited units like BESS. Although primary containment reserve accounts for energy management, it lacks detailed requirements for BESS to follow during the process. In GB, EFR was introduced in 2016 to enable faster frequency response from BESS and studies have highlighted the importance of careful SOC regulation for satisfactory outcomes [10]–[12]. Meanwhile, frequency quality can be compromised in certain cases due to improper SOC management [13].

In late 2020, National Grid Electricity Transmission (NGET), TSO of GB, developed a new suite of fast-acting frequency response services as a step-up form of EFR [14], with DCFR being the major service, requiring a full delivery time within 1 second. This makes DCFR more rapid than the aforementioned frequency regulation services. Additionally, the symmetric design and detailed energy recovery rules make BESS more suitable to deliver such a service. Therefore, as a frequency response service that is applicable to any power system, an evaluation of BESS providing DCFR in terms of frequency quality and SOC management is a valuable

TABLE I
OVERVIEW OF PREVIOUS RESEARCH WORK RELATED TO DCFR AND THIS WORK

Ref.	Focus on grid frequency regulation	BESS as subject	SOC management impact analysis	DCFR configuration constraints on BESS	Dynamic simulation between grid and BESS
[15]	√	×	×	×	×
[16]	√	×	×	×	×
[17]	√	×	×	×	×
[18]	√	√	×	×	×
[19]	√	√	×	×	√ (only focus on grid side)
[20]	√	√	×	×	×
[21]	√	√	×	×	×
[22]	×	√	×	×	×
[23]	×	√	×	×	√ (only focus on grid side)
This work	√	√	√	√	√

exploration. It has to be noted that DCFR is officially named as DC by NGET, however, it can be confusing to the readers since it conflicts with the terminology of direct current. Hence the term of DCFR is adopted in this paper.

Several studies have been conducted since DCFR was launched. Researchers in [15] combine both EFR and DCFR and compare them with traditional PFR in the event of sudden generation loss, while the authors of [16] compare DCFR with other newly proposed fast services and discuss their distinct roles. However, both [15] and [16] do not specify the technology used for providing such services. Ref. [17] evaluates the performance of a flywheel system when delivering DCFR, which provides limited guidance for BESS units. On the other hand, a few works explore the possibility of utilizing BESS as the provider of DCFR. A sensitivity study of BESS performing DCFR is undertaken in [18], while the authors of [19] compare PFR with DCFR for the effectiveness of improving frequency nadir when facing disturbance. However, the SOC management mechanism when delivering DCFR is not covered in neither research work. Article [20] proposes a strategy for BESS to better manage SOC levels for cost reduction, but this paper is short of the details of SOC management. An optimizing strategy for BESS-integrated wind farms to provide DCFR is introduced in [21], the strategy introduces SOC management rules but without discussing its impact on BESS performance. Moreover, the article concentrates on the storage optimization and power exchange between a wind farm and BESS. Hence, the complete exploration of DCFR SOC management impact has not yet been discussed. Furthermore, the studies in [18]–[21] lack the analysis on the configuration constraints implicitly imposed by the DCFR energy recovery rules, a factor that significantly influences BESS performance. Additionally, these studies either rely on acquired frequency data or simply incorporate a random power loss in the system model, neglecting the dynamic interplay between grid frequency and BESS. Aside from frequency regulation, certain investigations also center on the impact of DCFR on other aspects such as local voltage or transient rotor angle stability of synchronous generators [22], [23]. Table I explicitly compares this work with the above literature related to investigation on DCFR.

Within the limited body of research on DCFR, there is a notable research gap in comprehensively understanding the overall operations of DCFR. The significant impact of SOC management rules on BESS performance also necessitates a thorough investigation of DCFR functionality. Besides, DCFR configuration constraints imposed by energy recovery requirements upon BESS have not been adequately addressed in previous studies. Furthermore, as an evolution product of previous EFR, a comparison between DCFR and EFR is yet to be discussed for better understanding DCFR characteristics.

Given that previous research on DCFR has largely overlooked the interactions between grid frequency and BESS input/output, a well-developed power system model is necessary to dynamically simulate such mutual effects on a adequate manner. Additionally, as the acquisition of model input with high resolution is challenging to achieve, an input estimation method is also needed for completing the investigation.

To address the identified gaps in the literature, this paper offers an in-depth exploration of the DCFR mechanism and operation as applied to BESS, with a focus on frequency regulation, SOC management, and the implications of configuration constraints. It also provides a stability analysis of the BESS system under various conditions. The main contributions of this study are:

1) **DCFR service exploration:** A comprehensive foundation of the BESS-based DCFR service is presented, covering power response characteristics, SOC management rules, and the associated service configuration constraints. This interpretation offers a perspective on the DCFR mechanism and its operational framework for BESS.
2) **SOC management impact analysis:** A stability analysis for BESS providing DCFR is conducted, assessing the impact from SOC management mechanism. Conditions to maintain a stable SOC management system are summarized, which are supported by case studies in the developed integrated power system model.
3) **Identification of key BESS configurations:** Carry out investigations to identify the key influential parameters of battery settings when providing DCFR. Furthermore, the study includes a comparative analysis between DCFR and its predecessor, EFR, to highlight the performance distinctions and improvements. The results offer guiding significance to DCFR operators.

This article is structured as follows: In Section II, the technical specification of DCFR service is analyzed and described in a detailed manner. BESS configuration constraints due to energy recovery rules are also discussed. In Section III, the impact of BESS on power system frequency is discussed. A corresponding power system model integrated with BESS SOC management system is subsequently developed. A stability analysis of the SOC management system is also carried out in this section. In Section IV, a power imbalance estimation method is introduced, and the service assumptions of DCFR are presented. In Section V, four parameters of BESS configurations that can affect DCFR service performance are analyzed individually. Finally, a comparison between DCFR and EFR is also carried out. Section VI concludes this work.

II. DCFR Service Technical Specifications

A. DCFR response characteristics

DCFR is developed to mitigate the risks associated with reduced grid inertia and volatile power imbalances in the power system [24]. NGET aspires to contract 1 GW of DCFR service [25], with a requirement for contracted quantity delivery within 1s of the frequency deviation [26], where the contracted quantity represents the maximum power of the service. BESSs are well-suited for providing DCFR due to their fast-responding capabilities. Fig. 1 shows the DCFR response characteristic, activation is triggered only when frequency is outside the deadband (49.985, 50.015 Hz). Positive power output indicates energy injection during low-frequency situations, while negative power output signifies energy absorption from the system during over-frequency conditions. The knee-points (49.8, 50.2 Hz) require a BESS to provide 5% of the contracted quantity, while the remaining 95% is allocated further until saturation points (49.5, 50.5 Hz). Thus, DCFR, as a frequency regulation service, accommodates all frequency situations but prioritizes significant deviations.

It is noteworthy that DCFR reserve capacity can be partially or asymmetrically provided. DCFR high-frequency (DCFR-HF) involves offering the service exclusively during over-frequency situations, while DCFR low-frequency (DCFR-LF) focuses on under-frequency events. A bundled service can deliver frequency regulation in both directions but reserve capacity may be asymmetrical.

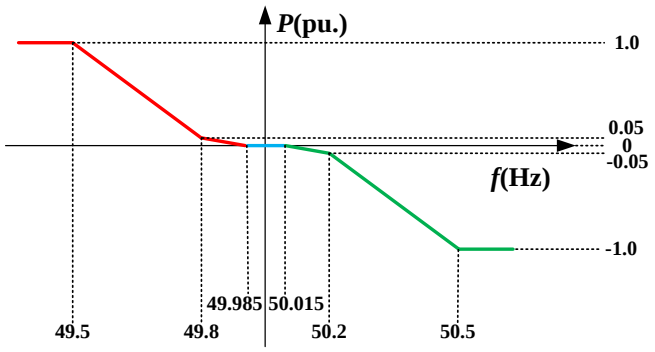

Fig. 1. DCFR power-frequency response characteristics

B. DCFR SOC management mechanism

The previous fast frequency service, EFR, implements a SOC management strategy by introducing multiple response curves (see [13]). In contrast, DCFR, as an evolved service, follows a single-curve line as SOC management is detached from the power response. BESS manages SOC through the submission of an operational baseline in each Settlement period (SP). SP is a half-hourly time interval during which electricity consumption and generation are measured and recorded in GB electricity market, as shown in Fig. 2. The operational baseline represents the power output solely dedicated to managing energy levels and remains constant throughout each SP. The actual power output from BESS is the sum of the operational baseline and real-time frequency response power (Equation (1)). $P_{BESS}(t)$, $P_{FR}(t)$ and $P_{SOC}(t)$ respectively denote the total power, frequency response power, SOC management power via baseline. The difference between the metered power output and the submitted baseline will be evaluated by NGET; failure to comply with the response delivery requirements may result to penalization.

$$P_{BESS}(t) = P_{FR}(t) + P_{SOC}(t). \tag{1}$$

It's important to note two features of the operational baseline: Firstly, there are ramp rate limits when transitioning between two SPs, with a maximum limit of 5% of the contracted quantity per minute. Single-side DCFR suppliers have ramp rate limits in one direction only. Secondly, there is a 1-hour gate closure before baselines can be applied due to the convention in the balancing market [26]. BESS-based DCFR service providers calculate their SOC levels at the start of each SP and submit the corresponding baseline by the end of that SP. The baseline will then take effect after two consecutive SPs. Thus, it will take 90 minutes for the baseline to be applied. Fig. 2 depicts the functionality of DCFR SOC management.

Fig. 3 demonstrates the generation of total power output by a BESS providing DCFR service. P^r_{BESS}, P^r_{FR} and P^r_{SOC} are the rated power, contracted quantity and maximum baseline of BESS. Q^r_{BESS} represents the rated capacity of BESS, and K represents the ratio of P^r_{SOC} to P^r_{BESS}, indicating the headroom power reserved for SOC management.

The operational baseline can be calculated via presetting the SOC management target (SOC_t), as shown in equation (2). SOC_{SP} is the settlement period SOC, which indicates the measured SOC level at the beginning of every SP, and P_{SOC} is the corresponding baseline power to be implemented 90 minutes later. t_{SP} is the time interval of each SP, which is 30 minutes.

$$P_{SOC} = \frac{SOC_t - SOC_{SP}}{t_{SP}} * Q^r_{BESS}. \tag{2}$$

C. BESS-based DCFR configuration constraints

As part of the SOC management mechanism, NGET imposes the following mandatory energy requirements that influence BESS performance, as outlined in [26]:

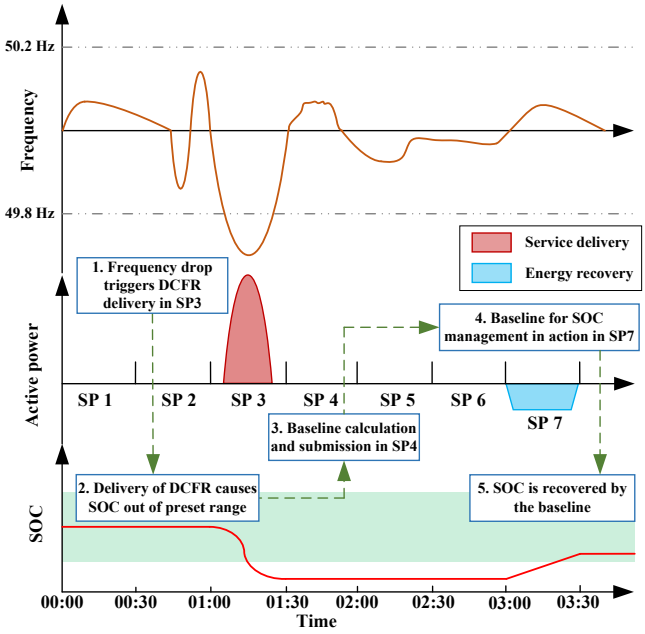

Fig. 2. DCFR SOC management mechanism in low-frequency situation [26] - top plot shows frequency variation; middle plot shows BESS power output responding to the frequency; bottom plot shows BESS SOC from the service delivery and energy recovery. This figure only presents service delivery when frequency is outside of knee-point range as an example

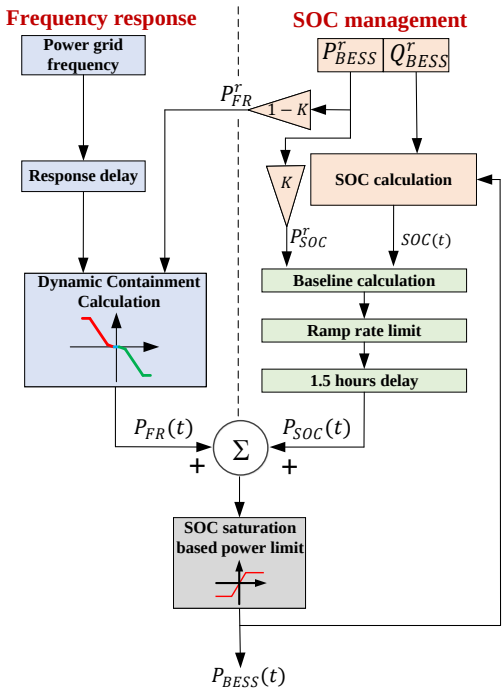

Fig. 3. Power calculation of DCFR service - dynamic BESS power consists of power from service delivery and SOC management

- Response energy volume (REV): the minimum energy a BESS should be able to deliver before SOC management is applied. It is calculated as 15 minutes of the full contracted quantity, shown in equation (3).
- Energy recovery (ER): the minimum energy recovered from SOC management in each SP. It is calculated as 20% of REV, shown in equation (4). Since it is a minimum energy requirement, it is also the lower energy provision limit from baselines in 30 minutes.

$$REV = P^r_{FR} * t_{REV}, \tag{3}$$

$$ER = REV * 0.2 \leq P_{SOC}(t) * t_{SP}, \tag{4}$$

where t_{REV} is the required time interval which is 15 minutes. Therefore, given P^r_{SOC} is the maximum baseline ($P^r_{SOC} \geq P_{SOC}(t)$) the relationship between contracted quantity and maximum baseline can be derived in equation (5) and subsequently leads to the final formulation in equation (6).

$$P^r_{SOC} * t_{SP} \geq REV * 0.2 = P^r_{FR} * t_{REV} * 0.2, \tag{5}$$

$$\frac{P^r_{FR}}{P^r_{SOC}} = n \leq \frac{5 * t_{SP}}{t_{REV}} = 10. \tag{6}$$

Equation (6) reveals that the SOC management ratio n should be no more than 10 for BESS providing DCFR service, indicating the power reserved for SOC management should be at least 10% of the power reserved for frequency response. Other than the SOC management ratio, the energy requirement also imposes a limitation to the C-rate and SOC management range of BESS. C-rate represents the ratio of rated power to the rated capacity of a battery shown in equation (7).

$$C = \frac{P^r_{BESS}}{Q^r_{BESS}}. \tag{7}$$

SOC management range refers to the scope where SOC needs to be managed once falling outside, which spans from lower limit (SOC_l) to upper limit (SOC_h). REV specifies the minimum stored energy before SOC management takes place, hence SOC range should provide a higher threshold than REV, shown in equation (8). It presents that the lower limit of SOC management range should contain at least the energy of REV; the upper limit works the same way reversely.

$$Q^r_{BESS} * SOC_l \geq REV. \tag{8}$$

Given t_{REV} equals to 15 minutes and the energy unit is MWh, equation (6)-(8) can be combined as equation (9).

$$C \leq \frac{4 * SOC_l * (n+1)}{n}. \tag{9}$$

For example, a system with $n = 10$ will result in a C-rate no more than 4.4*SOC_l, and if the lower limit of SOC management range is set at 40%, then $C_{max} = 1.76$, which means the value of rated power of BESS should not be more than 1.76 times of the value of rated capacity. The smaller C-rate should be used if the SOC management range is asymmetrical.

III. MODELING THE POWER SYSTEM WITH BESS INTEGRATION

A. Swing-equation model for system frequency

System frequency can be mathematically derived through the swing equation below [27]

$$2H * \frac{d \triangle f(t)}{dt} + D * \triangle f(t) = P_g(t) - P_d(t), \tag{10}$$

where H is the equivalent system inertia constant, D is the self-regulating load response, $\triangle f(t)$, $P_g(t)$ and $P_d(t)$ are the frequency deviation, power generation and power demand in per unit manner. It is clear that the more unbalanced the system, the greater the frequency deviation.

Equation (11) describes how frequency deviation is determined by power imbalance in the Laplace domain.

$$\triangle f(s) = \frac{P_g(s) - P_d(s)}{(2Hs + D)}. \tag{11}$$

The swing equation is adjusted by including a BESS that aims to minimize the power imbalance, as presented in equation (12). BESS power can be expressed in a simplified manner in equation (13), where k and b are the slope and intercept of the DCFR response curve.

$$2H * \frac{d \triangle f(t)}{dt} + D * \triangle f(t) = P_g(t) - P_d(t) + P_{BESS}(t), \tag{12}$$

$$P_{BESS}(t) = (k * \triangle f(t) + b) * P^r_{FR}. \tag{13}$$

As the intercept b and SOC management power do not contribute to frequency response, they are excluded from the swing equation. Hence, the modified frequency deviation equation in Laplace domain will eventually result in

$$\triangle f(s) = \frac{P_g(s) - P_d(s)}{(2Hs + D - k * P^r_{FR})}. \tag{14}$$

Comparing equation (14) and (11), the part of $-k * P^r_{FR}$ in the denominator is the impact brought by the BESS. Since k is a non-positive value from the DCFR response curve, the denominator gets greater thanks to BESS contribution, resulting in a smaller frequency deviation. Hence, the provision of DCFR by BESS yields a favorable impact on system frequency.

B. Power system model development

Using GB power system as an example, a corresponding model is developed based on the swing equation, as shown in Fig. 4, to incorporate system inertia, PFR, SFR, and DCFR service provided by BESS. The model takes power imbalance as input and determines system frequency in each simulation cycle. The calculated system frequency also feeds back to PFR, SFR, and BESS blocks for determining the corresponding frequency response power. Such dynamics are not accounted for in the existing literature. PFR and SFR are provided by conventional power plants with droop and integral control signals, respectively. BESS operate in parallel with PFR and SFR, providing dynamic containment service. The combined power output from frequency response minimizes the power imbalance, resulting in a smaller frequency deviation. Model parameters are listed in Table II, developed based on the following assumptions:

TABLE II
GB POWER SYSTEM PARAMETERS

System & turbines					
H (s)	*D (pu)*	T_T (s)	T_G (s)	T_{D1} (s)	T_{D2} (s)
3.62	1	0.3	0.2	8	20
Frequency response					
R (pu)	*k (pu)*	k_{SFR} (pu)	k_{PFR} (pu)	t_1 (s)	t_2 (s)
0.5	0.006	0.48	0.6	2	10

- System inertia constant (H) is determined based on comprehensive assessments of renewables, gas, and other generation types using UK generation data in 2020 February [28] and the corresponding inertia constants [15].
- Damping constant D is set to 1.0. T_G and T_T depict the governor and turbines response, and transient droop compensator for stable frequency performance is represented by T_{D1} and T_{D2} [27].
- The model includes a deadband of $\pm$15 mHz for PFR and SFR activation [29].
- NGET requires the generator governor droop settings of 3% - 5% for primary frequency response, therefore the denominator of PFR gain R is set to 0.5 [30]. SFR is represented by integral control, of which the gain k is collected from another research [31].
- The ratio of generation that provides PFR is represented by k_{PFR}, which is derived from the electricity production by sources in the UK [28]. Since renewable generation accounts for around 40% and possesses little frequency regulation capability, k_{PFR} is then set at 0.6.
- The ratio of generation that provides both PFR and SFR is represented by k_{SFR}. It is assumed that 80% of generation that provides PFR also participates in the SFR market [15], hence k_{SFR} is assumed to be 0.48.
- The system model is developed based on the UK total power demand of 41 GW [32].

C. SOC management and stability analysis

The BESS model is integrated in the power system model in Fig. 4. As described in the above section, the total power output P_{BESS} is comprised of power for DCFR service (P_{FR}) and power for SOC management (P_{SOC}). The gain k_{DC} in the model represents the power-frequency characteristics shown in Fig. 1. BESS SOC calculation is described by an integral block, indicating the energy accumulated in the battery and k_{SOC} is the factor for normalizing the corresponding energy into percentage. SOC_t indicates the target level of SOC management, hence it is introduced as a disturbance in the model. Similarly, k_{OB} represents the operational baseline power which converts the energy recovery into corresponding power. It is highlighted that the energy requirement of DCFR imposes a minimum energy recovery level for SOC management and the maximum power is also subject to the n ratio as outlined in section II, indicating that the power may not correct SOC to its target level, hence k_{OB} is constrained in a

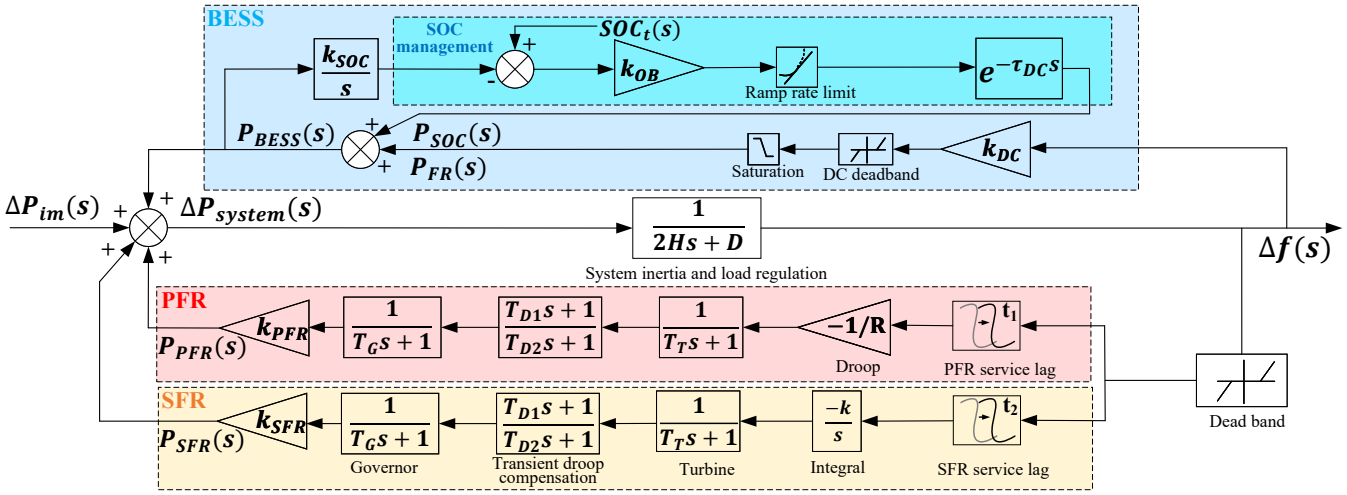

Fig. 4. GB power system model with BESS integration - PFR and SFR account for the associated deadband and service lags. BESS model consists of frequency response and SOC management. Ramp rate limit, saturation and DCFR deadband components are not included in the transfer function expression to provide a general scenario.

limited range. Finally, the operational baseline activation delay time of 90 minutes ($\tau_{DC} = 5400$) is implemented. Therefore, BESS power can be calculated via equation (15).

$$P_{BESS}(s) = \frac{k_{DC} * \Delta f(s) + k_{OB} * e^{-\tau_{DC}s} * SOC_t(s)}{1 + \frac{k_{SOC}}{s} * k_{OB} * e^{-\tau_{DC}s}}. \tag{15}$$

As an ancillary service provider, it is important to analyze the stability performance of BESS, especially for SOC management. According to Fig. 4, the open loop transfer function of SOC management can be obtained as given by equation (16). Note that the ramp rate limit, saturation and deadband blocks are not considered for stability analysis.

$$G(s) = \frac{k_{SOC}}{s} \cdot k_{OB} \cdot e^{-\tau_{DC}s}. \tag{16}$$

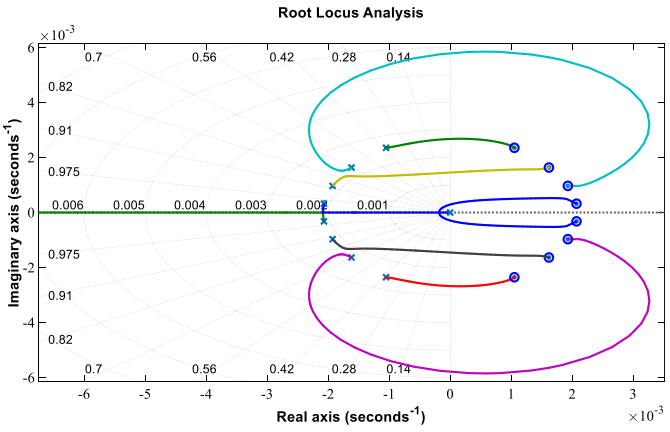

Fig. 5. Root locus result of SOC management, as gain increases, locus crosses imaginary axis, resulting in a unstable system.

The root locus of BESS model is therefore drawn in Fig. 5. It is worth noting that the delay component in equation (16) expressed via the Taylor series expansion results in an infinite number of characteristic roots, hence there is supposed to be an endless number of locus. This paper simplifies the expression by adopting only the first eight terms of the expansion, and only the locus related to the selected terms are demonstrated in the figure. Fig. 5 demonstrates that as the open-loop gain increases, the closed-loop characteristic roots tend to cross the imaginary axis and enter the right-side (unstable area) in the s-plane, indicating that the system will lose its stability if the gain is large enough to make the locus cross the axis. The open-loop gain of the root locus is a combination of k_{SOC} and k_{OB}, implying that the factors influencing these two gains are crucial in designing a stable SOC management system. The variable k_{SOC} represents the energy throughput of the charging/discharging process, determining the rate at which the SOC level changes corresponding to constant power, while k_{OB} denotes the operational baseline level, which is associated to SOC management process. This indicates that, for a stable SOC management system, the rate of energy accumulation during charging/discharging and the submitted operational baseline must be constrained within a limited range. Based on the description of Section II, the possible means to achieve a stable system would be: i) keeping an appropriate n ratio; ii) setting a reasonable recovery level; iii) avoiding frequent SOC management actions. These will be tested and discussed in the case studies.

It is speculated that the unstable issue is caused by the long delay time for SOC management command to be implemented. Therefore, it is also worth investigating further on the impact of such delay time. Fig 6 demonstrates the root locus of the same system with different delay time. Time delays of 60 minutes and 30 minutes are investigated apart from the default setting.

It can be observed that as the delay time reduces, the poles moves to farther left and zeros moves to farther right. Such behaviors change the system open-loop gain threshold to cross the imaginary axis. The critical level of the top locus for each system to cross is 0.0174, 0.0086 and 0.0060, which corresponds to a delay time of 30 minutes, 60 minutes and 90 minutes. The shown results imply that the system with a reduced time delay can handle larger open-loop gain without

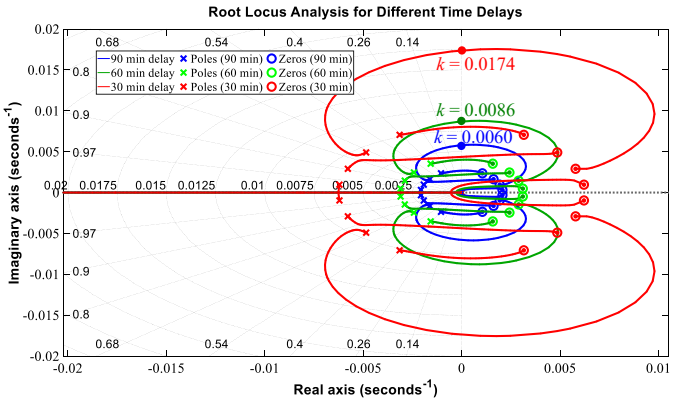

Fig. 6. Root locus result of SOC management with different delay time, as the delay time reduces the gain needed to cross the imaginary axis increases, indicating a more stable system.

losing the stability, indicating a more stable and robust system. Therefore, a decrease of the delay can support a stronger SOC management system of DCFR. The investigation of the delay time will also be conducted in a separate case study in the following section.

IV. SIMULATION SETUP

A. Power imbalance estimation

The power system model generates the system frequency with power imbalance as input, however, both generation and demand data are difficult to acquire with high time resolution due to the lack of second-based measurements. As a result, it is necessary to employ estimation methods to derive the model input. System frequency, as the product of system imbalance, can be measured with a much finer precision. Therefore, a power imbalance estimation method based on historic frequency data is illustrated in Fig. 7.

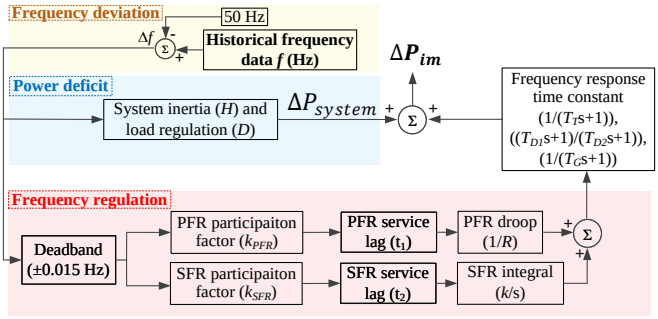

Fig. 7. Illustration of the power imbalance estimation method

The method consists of three parts, beginning with frequency deviation calculation, where historic frequency data will be compared with the nominal value. Then the frequency deviation will be subsequently fed into power deficit and frequency regulation blocks. The power deficit can be defined as the residual power imbalance left after the contributions from frequency response techniques, and it can be expressed in equation (17). This step reversely derives the imbalance level of the system after being regulated.

$$\triangle P_{system}(s) = \triangle f(s) * (2Hs + D). \tag{17}$$

Frequency regulation, on the other hand, works in parallel with power deficit calculation. This section separates the frequency contribution of PFR and SFR from $P_{system}(s)$, as system frequency is also the frequency response input. Equation (18) and (19) show the frequency response power from PFR and SFR if deadband and service lag requirements are met. Eventually the initial power imbalance of the system can be determined by equation (20).

$$\triangle P_{PFR}(s) = \triangle f(s) * k_{FR} * (\frac{-1}{R}) * \frac{1}{T_G s + 1} * \frac{T_{D1}s + 1}{T_{D2} + 1} * \frac{1}{T_T s + 1}, \tag{18}$$

$$\triangle P_{SFR}(s) = \triangle f(s) * k_{FR} * k_{SFR} * (\frac{k}{s}) * \frac{1}{T_G s + 1} * \frac{T_{D1}s + 1}{T_{D2}s + 1} * \frac{1}{T_T s + 1}, \tag{19}$$

$$\triangle P_{im}(s) = \triangle P_{system}(s) + \triangle P_{PFR}(s) + \triangle P_{SFR}(s). \tag{20}$$

This estimation method builds upon the approach proposed in [33]. However, the previous one was applied to a small system (the Danish island of Bornholm), where only PFR is considered. In contrast, this estimation method can be applied to larger-scale systems since it involves not only PFR and SFR, but also accounts for the associated requirements such as service lag time and deadband, which are not discussed in previous research studies. The estimated power imbalance data is validated by reusing it as the model input, with the resulting system frequency data subsequently compared with the historical data. The comparison results show that the correlation coefficient between the two frequency datasets is 99%, demonstrating the capability of the method to replicate the behaviors of a power system.

B. BESS configurations and DCFR service assumptions

One of the main objectives of this paper is to investigate the impact of different configurations of the battery and identify the corresponding challenges when providing DCFR. Therefore, the BESS used for the simulation is considered as an aggregated single large-scale BESS of all distributed participants, which allows for simplified modeling and analysis by considering the collective behavior. The DCFR contracted quantity of the BESS is set at 1 GW as planned by NGET. However, DCFR service also requires BESS to reserve certain space for SOC management, hence the rated power of BESS will be greater depending on n ratio. The ideal and initial SOC level is set at 50% as it offers the maximum room for both charging and discharging.

At the same time, since a large variety of DCFR options can be selected, which adds complexity to the analysis, the following assumptions are made throughout the simulations:

- There is no response delay as it is very small.
- DCFR service is provided as a bundled service with 1 GW in both directions.

TABLE III
SIMULATION STUDY CASES

Cases	C-rate	SOC management range	n ratio	SOC management target
Case study 1	1.76; 1.0; 0.5	40%-60%	10	Minimum ER
Case study 2	0.8	40%-60%; 30%-70%; 20%-80%	10	Minimum ER
Case study 3	1.68	40%-60%	10; 15; 20	Minimum ER
Case study 4	1.76	40%-60%	10	Minimum ER ; quarter line; middle line; edge line

- The ramp rate limit of baselines is assumed to be constant throughout each SP on a second-by-second basis, therefore the maximum ramp rate is calculated in equation (21) below.

$$(\frac{dP_{SOC}(t)}{dt})_{max} = \frac{P^r_{SOC}(t) * 5\%}{t_{SP}}. \quad (21)$$

V. INVESTIGATION AND RESULTS DISCUSSION

In this section, four BESS configuration parameters that influence SOC management are described and investigated: C-rate and SOC management range, ratio and target. The four cases are shown in Table III, with several scenarios assigned to each case. Moreover, two additional case studies are also conducted to discuss the impact of delay time and to compare DCFR with EFR. Simulations are conducted for a 2-day time period between 22$^{\text{nd}}$ and 24$^{\text{th}}$ February 2020 using GB power system. This period is chosen because of high frequency volatility and numerous under-frequency events. The corresponding historical frequency data can be obtained in [34].

Since SOC level is one of the investigation focuses, the associated battery degradation is also considered. Battery cycle degradation, which is the degradation type caused by active charging and discharging, is assumed to be proportional to Full equivalent cycles (FEC) [35]. FEC refers to the number of complete charge and discharge cycles during operation and it is calculated in equation (22) below, where $E^{im}(t)$ and $E^{ex}(t)$ are the energy import and export of BESS.

$$FEC(t) = \frac{\Sigma(E^{im}(t) + E^{ex}(t))}{2\ Q^r}. \quad (22)$$

A. Case study 1: C-rate investigation

Different C-rates of BESS are compared in the simulation, with corresponding settings in Table IV and results in Fig. 9. According to the previous analysis in Section II, $C = 1.76$ is the maximum C-rate when $n = 10$ and SOC management range is 40%-60%. P^r_{FR} and P^r_{SOC} remain constant with a fixed n ratio, while Q^r varies based on the specific C-rate.

TABLE IV
BESS CONFIGURATIONS WITH DIFFERENT C-RATES

C-rate	P^r_{FR} (MW)	P^r_{SOC} (MW)	P^r (MW)	Q^r (MWh)
1.76	1000	100	1100	625
1.0	1000	100	1100	1100
0.5	1000	100	1100	2000

* n = 10, and SOC pre-set range is 40% - 60%.

SOC exhibits significant oscillations at the highest C-rate due to the 90-minute delay in SOC management actions. Fig. 8 illustrates the energy and SOC evolution for the $C = 1.76$ scenario during a 12-hour period on February 22$^{\text{nd}}$. Energy plots include energy provision for frequency response, SOC management, and the overall combined results. SOC plots display dynamic SOC variation and settlement period SOC (the value measured at the start of each SP). At 12:30, indicating the start of the 25$^{\text{th}}$ SP, a low-SOC situation is detected. A baseline for SOC management is subsequently submitted at 13:00, and implemented two SPs later during the 28$^{\text{th}}$ SP at 14:00, causing a 90-minute delay.

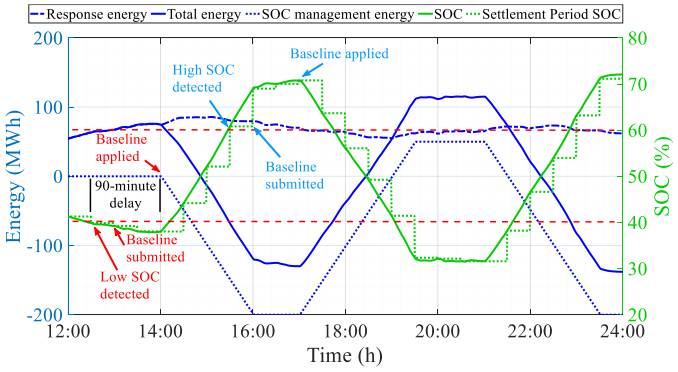

Fig. 8. $C = 1.76$ scenario - Energy and SOC simulation analysis for 12 hours on 22$^{\text{nd}}$ February 2020; red text refers to low SOC detection, while blue text refers to high SOC detection

It is important to emphasize that SOC measurement is continuous. If SOC falls outside the predefined range without bouncing back, detection occurs at the start of each SP within the next 90-minute period. In Fig. 8, SP 25, 26, 27, and 28 all detect low SOC, leading to corresponding baselines being implemented with a 90-minute delay in SP 28, 29, 30, and 31 respectively. The focus of Fig. 8 primarily highlights the first SP that identifies SOC outside the range as an example. Consequently, the delayed baselines result in excessive SOC management, causing SOC to breach the upper limit. This, in turn, triggers additional baselines submission to reduce SOC. However, such baselines for SOC reduction are also subject to delays, leading SOC to drop below the lower limit, initiating an oscillating cycle. Therefore, decreasing the time delay of SOC management action can significantly mitigate oscillation.

In comparison to the $C = 1.76$ scenario, the other two scenarios show no SOC oscillation. Lower C-rates indicate a larger battery capacity, as shown in Table IV, allowing for greater energy storage to reduce the likelihood of triggering SOC management. This behavior is also evident in Fig. 9 (a) and (c) in terms of power output, where higher C-rates activate power for SOC management more frequently. This oscillation also supports the stability analysis findings in section III.C,

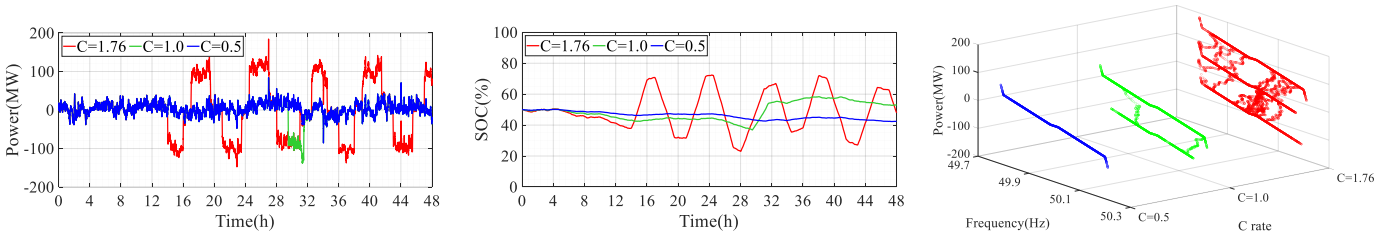

(a) Power output (b) SOC behaviors (c) Frequency vs power output

Fig. 9. Case study 1 BESS performance comparison - higher C-rate causes more serious SOC oscillation

where the lower C-rate reduce the need of frequency SOC management. In the cases of no SOC management, such SOC feedback loop component is removed in the BESS model in equation (16), making the root locus result in the left-side of s-plane and increasing the stability.

The overuse of SOC management power also leads to high energy throughput and extreme SOC fluctuations, as shown in Table VI. The $C = 1.76$ scenario exhibits four times greater energy throughput and a wider SOC span compared to the other scenarios. This energy throughput significantly impacts battery degradation, measured by FEC. The $C = 1.76$ scenario shows FEC values over 6 times and 16 times higher than the $C = 1.0$ and $C = 0.5$ scenarios, respectively. Considering the proportional relationship between FEC and cycle degradation, the battery with $C = 1.76$ experiences cycle degradation at rates 6 times and 16 times faster.

In general, the negative effects of high C-rates caused by SOC management delays necessitate a larger capacity BESS for DCFR service. However, larger battery capacity implies increased investment and maintenance costs, reducing financial benefits. Hence, it is crucial to determine an appropriate C-rate that ensures overall satisfaction.

B. Case study 2: SOC management range investigation

The impact of SOC management also varies with different preset ranges. Fig. 10 illustrates the performance of three scenarios with different ranges, from narrow to wide. For all scenarios, the C-rate is set to 0.8 due to the configuration constraints from equations (7) and (8). P^r_{FR} and P^r_{SOC} remain constant at 1000 MW and 100 MW, respectively, resulting in a battery capacity Q^r of 1375 MWh.

A wider range reduces the need of triggering SOC management, thereby mitigating the impact of SOC management delays. In Fig. 10 (a) and (b), the baseline is submitted only once for the 40% - 60% range scenario due to the larger capacity. Importantly, SOC fluctuations remain within the wider range for the other two scenarios, thus avoiding the need of SOC management. As a result, the behaviors of the BESS in these two wider-range scenarios are identical, with overlapping curves. Similar to case study 1, the stability of BESS model is improved with wider range due to the removal of SOC feedback loop component in the transfer function in equation (16).

In this case study, FEC-based battery degradation in the 40% - 60% range scenario is only 1.35 times greater than the other two scenarios, as SOC management is triggered only once. However, such a small difference is influenced by the low C-rate value chosen specifically for investigating the SOC management range. In practical applications, higher C-rate settings are often preferred, highlighting the need for proper SOC management to ensure a constant supply of DCFR provision. Therefore, selecting a suitable range is vital to accommodate overall battery configurations.

C. Case study 3: SOC management ratio investigation

Since SOC management significantly impacts power output, this case study investigates the impact of SOC management ratio. In Section II, n_{max} is set to 10, with P^r_{SOC} required to be at least 10% of P^r_{FR}. However, reducing P^r_{SOC} further can alleviate the impact of SOC management delay, while keeping C-rate and SOC management range at a challenging level. Table V shows the selected scenarios, with n increased to 15 and 20. As P^r_{FR} remains constant at 1000 MW, P^r_{SOC} varies with n, along with the associated battery capacity Q^r_{BESS}.

TABLE V
BESS CONFIGURATIONS WITH DIFFERENT SOC MANAGEMENT RATIOS

n ratio	P^r_{FR} (MW)	P^r_{SOC} (MW)	P^r (MW)	Q^r (MWh)
20	1000	50	1050	596.59
15	1000	66.67	1066.67	606.06
10	1000	100	1100	625

* C = 1.76, and SOC pre-set range is 40% - 60%.

Fig. 11 illustrates the battery behavior of the three scenarios. Both the $n = 10$ and $n = 15$ scenarios exhibit SOC oscillations. However, compared to $n = 10$ scenario, the oscillation is mitigated when n is higher ($n = 15$) due to less power allocated for SOC management. This can be observed in Fig. 11 (a), where the first baseline is activated before the 16^{th} hour, a higher n ratio corresponds to less power for SOC management. Decreased SOC management power indicates a reduced negative impact caused by the 90-minute time delay. For the BESS system stability, the higher n ratio implies a smaller value of k_{OB} in equation (16), which result in a smaller open-loop gain of root locus, hereby leading the relevant closed-loop poles to the left side of imaginary axis and improve the stability.

Table VI shows that the $n = 10$ scenario results in energy throughput 1.7 times and 3.7 times higher than the other two scenarios, with no improvement on frequency quality. It also correspondingly translates to battery FEC values 1.66

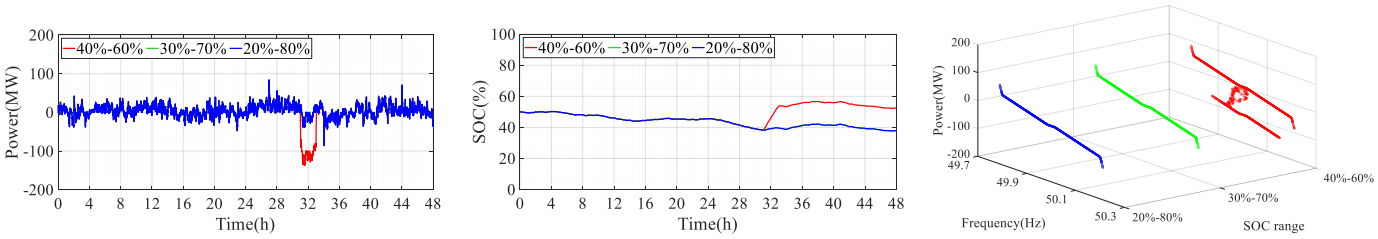

(a) Power output (b) SOC behaviors (c) Frequency vs power output

Fig. 10. Case study 2 BESS performance comparison - narrower SOC management range is more likely to trigger energy recovery action

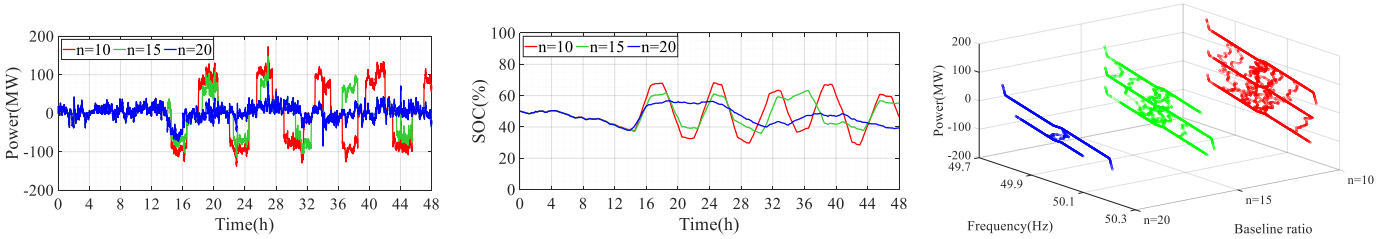

(a) Power output (b) SOC behaviors (c) Frequency vs power output

Fig. 11. Case study 3 BESS performance comparison - higher n ratio can levitate SOC oscillation impact

times and 3.51 times higher. Therefore, optimizing the SOC management power ratio when providing DCFR improves the service quality and sustains battery lifetime.

D. Case study 4: SOC management target investigation

Similar to case study 3, reducing SOC management power can be achieved by adjusting the SOC management target rather than adhering to the minimum energy requirement. In this approach, a factor of m is introduced for the calculation.

The SOC management target refers to the desired SOC level to which SOC is recovered at the end of the SP, determining the baseline power level. The energy recovery rules of DCFR aims to recover at least 20% of the REV per SP, serving as the benchmark for the case studies. However, this energy requirement is excessively high during normal frequency situations due to the 90-minute delay, as indicated by previous results. Therefore, alternative SOC management targets are proposed for investigation, including the quarter line, middle line, and edge line. These targets aim for specific levels within the SOC management range.

For instance, the middle line sets the SOC level at the midpoint between the SOC lower limit and the initial SOC level in low SOC situations or between the SOC upper limit and the initial SOC level in high SOC situations. For a BESS with a 40% - 60% SOC management range, this corresponds to 45% and 55%, respectively, with $m = 0.5$. The quarter line represents the SOC level set at 25% between the range limit and the initial SOC level, closer to the limit. In the above example, the targets change to 42.5% and 57.5%, respectively, with $m = 0.25$. Finally, the edge line requires the SOC to be recovered exactly at the range limit, resulting in $m = 0$. Thus, $m \subseteq [0, 1]$, and a smaller m value indicates less power requirement. Equation (23) demonstrates how the SOC management target is calculated for a specific m factor:

$$SOC_t^l = (SOC_n - SOC_l) * m + SOC_l, \tag{23a}$$

$$SOC_t^h = SOC_h - (SOC_h - SOC_n) * m, \tag{23b}$$

where SOC_l and SOC_h are the lower and upper limit of SOC management range, SOC_t^l and SOC_t^h denote the SOC management target in low SOC and high SOC situations respectively and SOC_n represents the ideal SOC set at 50%. It should be noted that the minimum energy recovery target required for DCFR service is considered as the maximum baseline power in this case. Therefore, any calculated power exceeding this level will be limited to $\frac{ER}{t_{SP}}$. Other parameters are set to the most challenging values, with $C = 1.76$, $n = 10$, and the SOC management range between 40% and 60%.

Figure 12 and Table VI compare the performance of the four scenarios. The minimum energy scenario, serving as the benchmark, exhibits the strongest SOC management action, followed by the middle line scenario. Neither the quarter line nor the edge line scenario triggers SOC oscillation due to their minimal demand for SOC management. Such phenomenon also supports the conducted stability analysis of BESS SOC management, the system stability is improved with adjusted SOC management targets that reduce the value of k_{OB} in equation (16), making the corresponding closed-loop characteristic roots on the left side of the imaginary axis.

From a statistical perspective, the minimum energy scenario results in energy throughput and FEC values 1.06 times, 4.02 times, and 3.69 times higher than the middle line, quarter line, and edge line scenarios, respectively. Thus, effectively adjusting SOC management targets helps mitigate the negative effects caused by the 90-minute time delay.

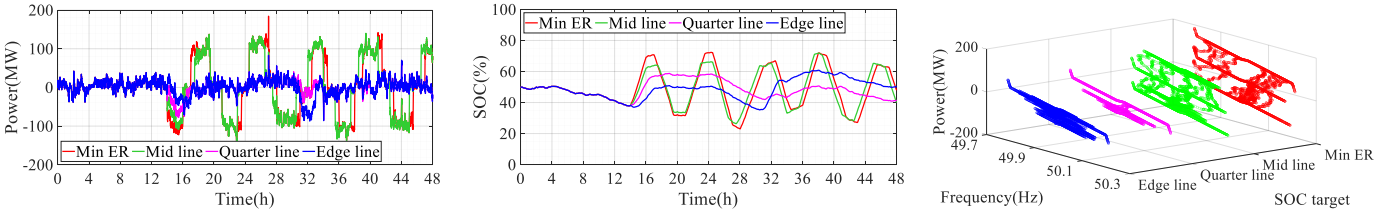

(a) Power output (b) SOC behaviors (c) Frequency vs power output

Fig. 12. Case study 4 BESS performance comparison - adjusting SOC management target helps mitigate SOC oscillation issues

TABLE VI
SIMULATION STATISTICAL RESULTS - DCFR INVESTIGATIONS

Cases	Scenarios	min SOC (%)	max SOC (%)	min frequency (Hz)	max frequency (Hz)	energy export (MWh)	energy import (MWh)	FEC
Case study 1	C=0.5	42.313	50.116	49.789	50.211	345.812	181.085	0.120
	C=1.0	36.839	58.336	49.789	50.211	330.254	363.659	0.315
	C=1.76	23.006	72.364	49.785	50.211	1253.734	1240.060	1,995
Case study 2	20%-80%	37.700	50.185	49.789	50.211	345.812	181.085	0.192
	30%-70%	37.700	50.185	49.789	50.211	345.812	181.085	0.192
	40%-60%	38.256	56.675	49.789	50.211	338.919	374.253	0.259
Case study 3	n=20	37.869	56.788	49.790	50.211	336.405	271.692	0.485
	n=15	35.846	63.231	49.790	50.211	639.149	668.315	1.025
	n=10	28.486	68.227	49.790	50.211	1130.390	1100.413	1.704
Case study 4	Edge line	35.262	60.791	49.790	50.211	337.027	338.254	0.540
	Quarter line	37.869	58.777	49.790	50.211	335.594	283.083	0.495
	Middle line	26.332	71.818	49.787	50.191	1199.315	1133.945	1.867
	Minimum ER	23.006	72.364	49.785	50.211	1253.734	1240.060	1.995

E. Case study 5: Operational baseline delay time discussion

In this case study, time delays of 90 minutes, 60 minutes, and 30 minutes, as analyzed in the stability study, are investigated. Additionally, a 15-minute delay is also included to further explore the impact of shorter delays. During the simulation, the BESS is set up with a demanding configuration, with C=1.76, n=10, SOC management range set as 40%-60% and the energy recovery aligned with the minimum scenario. When SOC management is required, a reduced delay time can help the battery to make swift actions, hence mitigating the issue of SOC oscillation, as demonstrated in Fig. 13. It is interesting that the extent of power fluctuation in case study 5 is similar among the different delay time scenarios, which differs from the results in study 3 and 4, as shown in Fig. 13 (a). It represents that the SOC management request via the submitted operational baseline remains constant regardless of the delay time, however, the decreased responding time help prevent excessive management of SOC, thereby reducing the need for subsequent requests to correct the SOC levels.

The SOC plot in Fig. 13 (b) provides further validation that SOC oscillation issue is significantly tackled when the delay time reduces to 60 minutes and further mitigated with 30 minutes and 15 minutes. It demonstrates the impact of operational baseline delay time on the behaviors of the BESS.

F. Case study 6: DCFR vs EFR

As the predecessor of DCFR service [14], EFR was developed into two types - service 1 and service 2, where service 1 focuses on SOC management, while service 2 prioritizes frequency regulation [13]. This case study compares DCFR with EFR for understanding its characteristics.

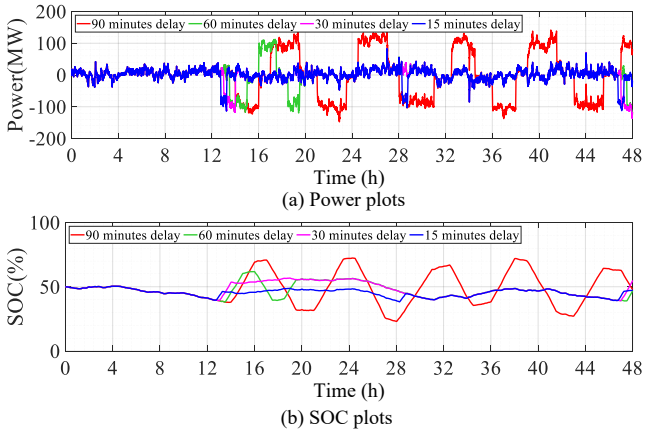

(a) Power plots

(b) SOC plots

Fig. 13. Case study 5 BESS performance comparison - reduced time delays mitigate SOC oscillation issues.

BESS configurations for both services are presented in Table VII, with DCFR settings aligned to the required n ratio and SOC management target. A narrow SOC range is selected to maximize the differences, and a C-rate of 1.0 is chosen to mitigate the negative impact of baseline delay. The maximum power for frequency regulation is set at 1000 MW.

TABLE VII
BESS CONFIGURATIONS FOR DCFR AND EFR

Services	SOC management range	C-rate	P^r (MW)	Q^r (MWh)
EFR	40%-60%	1.0	1000	1000
DCFR	40%-60%	1.0	1100	1100

* For DCFR, $n = 10$, hence $P^r_{FR} = 1000MW$ and $P^r_{SOC} = 100MW$; SOC management target is set to be the minimum energy requirement.

TABLE VIII
SIMULATION STATISTICAL RESULTS - DCFR VS EFR INVESTIGATIONS

Services	min SOC (%)	max SOC (%)	min frequency (Hz)	max frequency (Hz)	energy export (MWh)	energy import (MWh)	FEC
EFR service1	36.936	58.909	49.848	50.144	713.618	755.959	0.734
EFR service2	13.360	63.086	49.844	50.137	1471.175	1377.418	1.424
DCFR	36.839	58.336	49.789	50.211	330.254	363.659	0.315

Fig. 14 (a) shows the frequency comparison between DCFR and EFR services. All three services reduce frequency deviation compared to basecase frequency, which is the simulated system frequency without BESS integration. Meanwhile, the most stable SOC curve is achieved by DCFR according to Fig. 14 (b).

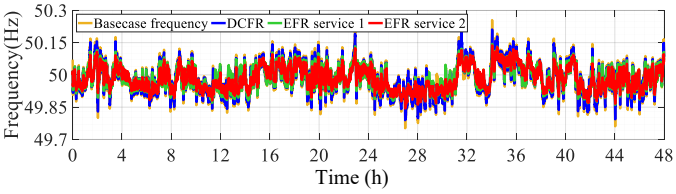

(a) Frequency plots

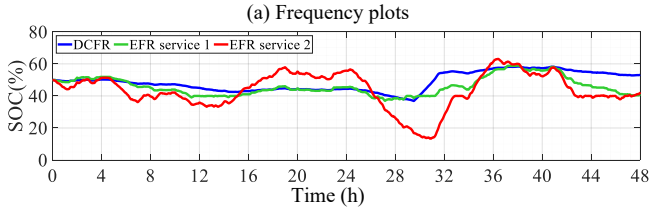

(b) SOC plots

Fig. 14. DCFR vs EFR comparison - all services help improve frequency quality, DCFR achieves the most stable SOC variation compared to EFR

Additionally, DCFR improves frequency quality by increasing the number of frequency data within the deadband, as shown in Fig. 15. EFR service 1 and service 2 sacrifice some frequency data for SOC management, resulting in fewer frequency data within the deadband. In contrast, DCFR implements an alternative SOC management mechanism and enhances the frequency quality. On average, DCFR service leads to a 7.93% higher percentage of frequency data within the deadband compared to the two EFR services. This indicates reduced activation of PFR and SFR, which is advantageous for financial benefits. Table VIII provides statistical comparisons among the services.

Although DCFR has a slightly wider frequency span than EFR, its SOC span is as narrow as EFR service 1. Moreover, the DCFR energy throughput is only 43.5% and 24.4% compared to EFR, corresponding to 42.9% and 22.1% of FEC, respectively. This shows that DCFR outperforms EFR by utilizing less energy while achieving similar frequency and superior SOC and FEC outcomes.

It should be noted that battery configurations can be further optimized to fully unlock the potential of DCFR. Since a significant portion of the DCFR response curve is designed for frequencies outside the knee-point range, DCFR may play a more crucial role in large frequency deviations in contingency situations. Moreover, the collective impact from both DCFR and other future ancillary services is also worth investigating,

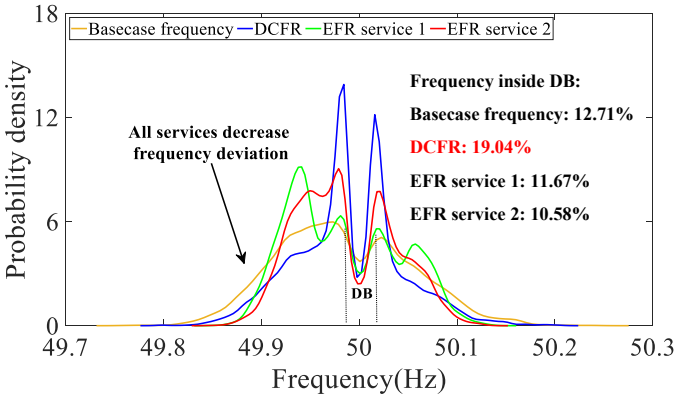

Fig. 15. Frequency probability density for DCFR and EFR - DCFR leads EFR by achieving more frequency data inside PFR/SFR deadband

particularly via experimental validation, this will be explored in the future research analysis.

VI. CONCLUSION

This paper provides an assessment and analysis of DCFR frequency response service, including the response curve, the SOC management rules, and the associated unit configuration constraints. A methodology is presented to investigate the performance of DCFR-based BESS in a power system, alongside a stability analysis focusing on the impact of the SOC management mechanism. The stability assessment is conducted via root locus study, where the theoretical findings show that large open-loop gains could cause instability to BESS SOC management system due to the long delay time. The results are supported by a comparative stability study aiming for different time delays, which demonstrates that the reduced delay enables the SOC management system to handle larger open-loop gains without losing the stability. Furthermore, four BESS configuration parameters that are relevant to the value of such gains in BESS SOC management system are identified via dynamic simulations for the service performance: C-rate, SOC management range, ratio and target.

A power imbalance estimation method is utilized for gaining the simulation input for the integrated power system model. The simulation results show that DCFR can improve frequency quality, but SOC management affects the power output significantly due to its 90-minute time delay and it might cause SOC oscillation if the battery is configured improperly. Low C-rate and wide SOC management range are less likely to cause SOC oscillation and low FEC, as they can alter the value of open-loop gains of the transfer function of SOC management system. Two other parameters are also analyzed: SOC management ratio and SOC management target. Low

SOC management ratio generates SOC oscillation and causes high FEC. Meanwhile, the impact can be alleviated by reconfiguring the SOC management target, the minimum energy recovery requirement ends up with more serious SOC fluctuation and high FEC than adjusted SOC management target scenarios. Both methods affect the stability of the SOC management system by changing the value the open-loop gain, hence avoiding the oscillation. A case study is dedicated for the time delay, the findings showcase that the SOC oscillation can be mitigated with reduced time delay even the BESS is set up with demanding configuration. Finally DCFR service is also compared with EFR, the results present that it utilizes less than 50% of energy throughput and achieves the best SOC curve. DCFR also outperforms EFR by leading the share of frequency inside deadband by 7.93% on average.

References

[1] Department for Energy Security and Net Zero, "Energy trends march 2023," 2024. [Online]. Available: https://assets.publishing.service.gov.uk/media/667c1741aec8650b10090082/Energy_Trends_June_2024.pdf

[2] N. Li, C. Uckun, E. M. Constantinescu, J. R. Birge, K. W. Hedman, and A. Botterud, "Flexible operation of batteries in power system scheduling with renewable energy," *IEEE Transactions on Sustainable Energy*, vol. 7, pp. 685–696, 2016.

[3] J. Engelhardt, A. Thingvad, J. M. Zepter, T. Gabderakhmanova, and M. Marinelli, "Energy recovery strategies for batteries providing frequency containment reserve in the nordic power system," *Sustainable Energy, Grids and Networks*, vol. 32, p. 100947, 12 2022.

[4] J. Li, F. Yao, Q. Yang, Z. Wei, and H. He, "Variable voltage control of a hybrid energy storage system for firm frequency response in the u.k." *IEEE Transactions on Industrial Electronics*, vol. 69, pp. 13 394–13 404, 12 2022.

[5] V. Knap, S. K. Chaudhary, D. I. Stroe, M. Swierczynski, B. I. Craciun, and R. Teodorescu, "Sizing of an energy storage system for grid inertial response and primary frequency reserve," *IEEE Transactions on Power Systems*, vol. 31, pp. 3447–3456, 2016.

[6] D. Fernández-Muñoz, J. I. Pérez-Díaz, I. Guisández, M. Chazarra, and Álvaro Fernández-Espina, "Fast frequency control ancillary services: An international review," *Renewable and Sustainable Energy Reviews*, vol. 120, 3 2020.

[7] A. Thingvad, C. Ziras, G. L. Ray, J. Engelhardt, R. R. Mosbæk, and M. Marinelli, "Economic value of multi-market bidding in nordic frequency markets," in *2022 International Conference on Renewable Energies and Smart Technologies (REST)*, vol. I, 2022, pp. 1–5.

[8] J. Fleer and P. Stenzel, "Impact analysis of different operation strategies for battery energy storage systems providing primary control reserve," *Journal of Energy Storage*, vol. 8, pp. 320–338, 2016. [Online]. Available: http://dx.doi.org/10.1016/j.est.2016.02.003

[9] G. Kapoor and N. Wichitaksorn, "Electricity price forecasting in new zealand: A comparative analysis of statistical and machine learning models with feature selection," *Applied Energy*, vol. 347, 10 2023.

[10] F. Sanchez, J. Cayenne, F. Gonzalez-Longatt, and J. L. Rueda, "Controller to enable the enhanced frequency response services from a multi-electrical energy storage system," *IET Generation, Transmission and Distribution*, vol. 13, pp. 258–265, 2019.

[11] B. M. Gundogdu, S. Nejad, D. T. Gladwin, M. P. Foster, and D. A. Stone, "A battery energy management strategy for u.k. enhanced frequency response and triad avoidance," *IEEE Transactions on Industrial Electronics*, vol. 65, pp. 9509–9517, 2018.

[12] S. Canevese, D. Cirio, A. Gatti, M. Rapizza, E. Micolano, and L. Pellegrino, "Simulation of enhanced frequency response by battery storage systems: The uk versus the continental europe system," *Conference Proceedings - 2017 17th IEEE International Conference on Environment and Electrical Engineering and 2017 1st IEEE Industrial and Commercial Power Systems Europe, EEEIC / I and CPS Europe 2017*, pp. 1–6, 2017.

[13] X. Cao and N. Zhao, "A cooperative management strategy for battery energy storage system providing enhanced frequency response," *Energy Reports*, vol. 8, pp. 120–128, 2022. [Online]. Available: https://doi.org/10.1016/j.egyr.2021.11.092

[14] National Grid Plc, "New fast frequency product to boost national grid eso's response capability," 2019. [Online]. Available: https://www.nationalgrideso.com/news/new-fast-frequency-product-boost-national-grid-esos-response-capability

[15] M. Nedd, J. Browell, K. Bell, and C. Booth, "Containing a credible loss to within frequency stability limits in a low-inertia gb power system," *IEEE Transactions on Industry Applications*, vol. 56, pp. 1031–1039, 3 2020.

[16] S. Homan and S. Brown, "The future of frequency response in great britain," *Energy Reports*, vol. 7, pp. 56–62, 5 2021.

[17] A. J. Hutchinson and D. T. Gladwin, "Suitability assessment of flywheel energy storage systems for providing new frequency response services in the uk," in *2022 IEEE PES Innovative Smart Grid Technologies - Asia (ISGT Asia)*, 2022, pp. 495–499.

[18] A. Abdulkarim and D. T. Gladwin, "A sensitivity analysis on power to energy ratios for energy storage systems providing both dynamic firm and dynamic containment frequency response services in the uk," in *IECON 2021 – 47th Annual Conference of the IEEE Industrial Electronics Society*, 2021, pp. 1–6.

[19] K. Sasompholsawat and R. Preece, "Investigating frequency services to stabilise low inertia power systems," in *The 17th International Conference on AC and DC Power Transmission (ACDC 2021)*, vol. 2021, 2021, pp. 19–24.

[20] L. Ochoa-Eguilegor, N. Goitia-Zabaleta, A. González-Garrido, A. Saez-de Ibarra, H. Gaztañaga, and A. Hernandez, "Optimized market bidding of energy storage systems for dynamic containment service," in *2021 IEEE International Conference on Environment and Electrical Engineering and 2021 IEEE Industrial and Commercial Power Systems Europe (EEEIC / ICPS Europe)*, 2021, pp. 1–6.

[21] F. Fan, J. Nwobu, and D. Campos-Gaona, "Co-located battery energy storage optimisation for dynamic containment under the uk frequency response market reforms," *CSEE Journal of Power and Energy Systems*, 07 2023.

[22] S. Sommerville, G. A. Taylor, and M. Abbod, "Voltage fluctuations of battery storage systems providing fast frequency response services in the uk," in *2022 57th International Universities Power Engineering Conference (UPEC)*, 2022, pp. 1–6.

[23] Z. Zhang, S. Asvapoositkul, and R. Preece, "Impact of fast frequency response on power system transient stability," in *The 17th International Conference on AC and DC Power Transmission (ACDC 2021)*, vol. 2021, 2021, pp. 13–18.

[24] "Dynamic containment service terms," pp. 1–24, 2021. [Online]. Available: https://www.nationalgrideso.com/document/177106/download

[25] "Dynamic containment faqs," 2020. [Online]. Available: https://www.nationalgrideso.com/document/164391/download

[26] "Dynamic containment guidance document," 2021. [Online]. Available: https://www.nationalgrideso.com/document/175296/download

[27] P. Kundur, *Power System Stability And Control*, 1993.

[28] UK Government's Department for Business, Energy & Industrial Strategy., "Electricity production and availability from the public supply system (ET 5.4 - monthly)," 2023. [Online]. Available: https://www.gov.uk/government/statistics/electricity-section-5-energy-trends

[29] National Grid Plc, "Firm frequency response frequently asked questions," 2017. [Online]. Available: https://www.nationalgrideso.com/document/95581/download

[30] ——, "The grid code issue 5 revision 21," 2017. [Online]. Available: https://www.nationalgrid.com/sites/default/files/documents/8589935310-Complete%20Grid%20Code.pdf

[31] M. Cheng, J. Wu, S. J. Galsworthy, C. E. Ugalde-Loo, N. Gargov, W. W. Hung, and N. Jenkins, "Power system frequency response from the control of bitumen tanks," *IEEE Transactions on Power Systems*, vol. 31, pp. 1769–1778, 2016.

[32] National Grid Plc, "Report of the national grid investigation into the. frequency deviation and automatic demand disconnection that occurred on the 27th may 2008." 2009. [Online]. Available: https://www.nationalgrideso.com/document/220851/download

[33] M. Marinelli, K. Sevdari, L. Calearo, A. Thingvad, and C. Ziras, "Frequency stability with converter-connected resources delivering fast frequency control," *Electric Power Systems Research*, vol. 200, 11 2021.

[34] National Grid Plc, "System frequency." [Online]. Available: https://www.nationalgrideso.com/data-portal/system-frequency-data

[35] A. Thingvad, L. Calearo, P. B. Andersen, and M. Marinelli, "Empirical capacity measurements of electric vehicles subject to battery degradation from v2g services," *IEEE Transactions on Vehicular Technology*, vol. 70, pp. 7547–7557, 8 2021.